

Article

Dynamic Cost-Optimal Assessment of Complementary Diurnal Electricity Storage Capacity in High PV Penetration Grid

Samuel Matthew G. Dumlao  and Keiichi N. Ishihara 

Department of Socio-Environmental Energy Science, Graduate School of Energy Science, Kyoto University, Yoshidahonmachi, Sakyo-ku, Kyoto 606-8501, Japan; ishihara@energy.kyoto-u.ac.jp

* Correspondence: dumlao.samuelmatthew.k34@kyoto-u.jp

Abstract: Solar Photovoltaics (PV) is seen as one of the renewable energy technologies that could help reduce the world's dependence on fossil fuels. However, since it is dependent on the sun, it can only generate electricity in the daytime, and this restriction is exacerbated in electricity grids with high PV penetration, where solar energy must be curtailed due to the mismatch between supply and demand. This study conducts a techno-economic analysis to present the cost-optimal storage growth trajectory that could support the dynamic integration of solar PV within a planning horizon. A methodology for cost-optimal assessment that incorporates hourly simulation, Monte Carlo random sampling, and a proposed financial assessment is presented. This approach was tested in Japan's southernmost region since it is continuously increasing its solar capacity and is at the precipice of high PV curtailment scenario. The results show the existence of a cost-optimal storage capacity growth trajectory that balances the cost penalty from curtailment and the additional investment cost from storage. This optimal trajectory reduces the impact of curtailment on the energy generation cost to manageable levels and utilizes more solar energy potential that further reduces CO₂ emissions. The results also show that the solar capacity growth rate and storage cost significantly impact the optimal trajectory. The incorporation of the Monte Carlo method significantly reduced the computational requirement of the analysis enabling the exploration of several growth trajectories, and the proposed financial assessment enabled the time-bound optimization of these trajectories. The approach could be used to calculate the optimal growth trajectories in other nations or regions, provided that historical hourly temperature, irradiance, and demand data are available.

Keywords: energy storage; solar curtailment; optimization; scenario analysis; cost-optimal; diurnal storage; high PV penetration; growth trajectory; generation cost



Citation: Dumlao, S.M.G.; Ishihara, K.N. Dynamic Cost-Optimal Assessment of Complementary Diurnal Electricity Storage Capacity in High PV Penetration Grid. *Energies* **2021**, *14*, 4496. <https://doi.org/10.3390/en14154496>

Academic Editors: Eduard Bullich-Massagué and Mònica Aragüés-Peñalba

Received: 11 June 2021
Accepted: 19 July 2021
Published: 25 July 2021

Publisher's Note: MDPI stays neutral with regard to jurisdictional claims in published maps and institutional affiliations.



Copyright: © 2021 by the authors. Licensee MDPI, Basel, Switzerland. This article is an open access article distributed under the terms and conditions of the Creative Commons Attribution (CC BY) license (<https://creativecommons.org/licenses/by/4.0/>).

1. Introduction

1.1. Solar Photovoltaic and the Energy Transition

In October 2016, the conditions for the entry into force of the Paris Agreement were met, and it entered into force on 4 November 2016. Signatories to this agreement agreed to submit a national climate plan to mitigate climate change by reducing greenhouse gas emissions. Similarly, one of the United Nations Sustainable Development Goals, established in 2015, is focused on affordable and clean energy. These two global initiatives helped promote renewable energy, such as wind, solar, and biomass, in the energy mix of several nations. Consequently, countries such as Germany and Denmark and subnational jurisdictions such as California, Scotland, and South Australia, developed and promoted their “green energy transition” initiatives [1]. Aside from these major players, more than 150 countries have national targets for renewable energy in the power sector [2].

All these initiatives have contributed to the increasing solar photovoltaics (PV) installation in the world, which grew from 138 GW to 627 GW from 2013 to 2019 [2]. Several countries have now reached high solar PV penetration, and with it comes the problem of solar curtailment. In 2008, Denholm et al. [3], researchers from the US National Renewable

Energy Laboratory, noticed a peculiar impact on the shape of the demand after subtracting solar generation. The California Independent System Operator later coined the term “duck curve” to describe this phenomenon given that the shape of the net load resembles a duck as solar installation increases [4]. This curve highlights the necessary changes that the flexible generators have to perform. First, the flexible generators should be able to ramp up and down, and second, the minimum generation of these generators should be lower than the “belly” of the “duck curve.” Solar curtailment has to be implemented if either of these conditions is not satisfied. Curtailment generally happens when the flexible load is unable to reduce production to compensate for the high volume of solar energy.

Several countries with high variable renewable energy installation are already experiencing solar curtailment. The mismatch of PV supply and electricity demand and the limitation of other sources to respond to rapid changes limits the large-scale integration of solar PV [5]. Possible solutions involve transmission [1,6], energy storage [5,7], and demand-side management [8–10]. Alternative solutions involve increasing the flexibility of other sources [1,5] and installing PV to better match demand [7,11].

In jurisdictions with high PV installation, such as Germany, California, and South Australia, there is minimal solar curtailment, but Japan and Hawaii face unique situations [1]. The electricity grid of the former is well-interconnected with neighboring countries and states [1]; thus, they are capable of trading excess energy to their neighbors. For instance, Germany can sell their excess solar or buy nuclear energy depending on the needs of their grid. On the other hand, Japan and Hawaii are isolated island nations and states with no trading options during peak solar production. In these cases, energy storage plays a significant role in the continued increase in solar penetration.

1.2. Japan's Situation

The Japanese government recently reiterated its commitment to the projected energy mix for 2030, where fossil fuel-based generation will be reduced to 46%, and renewable energy will comprise 22–24%, to which solar energy will make a 7% contribution [12]. To achieve the solar mix target, Japan promotes innovative research and development, improvements in the Feed-in Tariff (FiT), and competitive procurement prices using the Top-Runner method.

The Kyushu region, located on the western tip of Japan, is leading the country's solar PV generation. Relative to the rest of the country, the region has higher solar potential and cheaper land cost, which has driven the growth of solar investment in the region. As of early 2021, the region has a total installed capacity of 10.1 GW, and construction of additional plants that will increase this capacity further to roughly 16 GW [13] by around 2027 is already approved. The share of solar PV generation has been steadily increasing. In 2017, 2018, and 2019, solar PV generation accounted for 8.5%, 9.2%, and 10.1% of the total yearly generation, respectively.

However, Kyushu remains heavily dependent on thermal generation despite the increased solar and nuclear penetration, as seen in Figure 1. In 2017, 2018, and 2019, thermal generation accounted for 70%, 61.1%, and 50.9% of the total yearly generation, respectively. The decrease is mainly attributed to the increase in nuclear generation. As of June 2018, Kyushu restarted four of its six nuclear power plants (NPP) with a total capacity of 4.140 GW [14]. The other two power plants were permanently decommissioned. There is still an increasing need for additional solar investment to further reduce the dependence on thermal power plants. However, in October 2018, Kyushu was forced to curtail some solar production for the first time. More curtailment occurred in March 2019.

In order to reduce curtailment, Kyushu utilizes its transmission lines and pumped hydroelectric energy storage (PHES). The Kanmon interconnection line connects the Kyushu region to the rest of the country via a 500 kV, 2380 MW transmission line [15]. The region also has three hydroelectric power plants (pure pump-storage) with a total generation capacity of 2.3 GW and 6 h of storage [16]. These were initially designed to store excess

energy from the nuclear power plant but are now used to store energy during peak solar production and generate energy to support the ramp rate of the thermal plants.

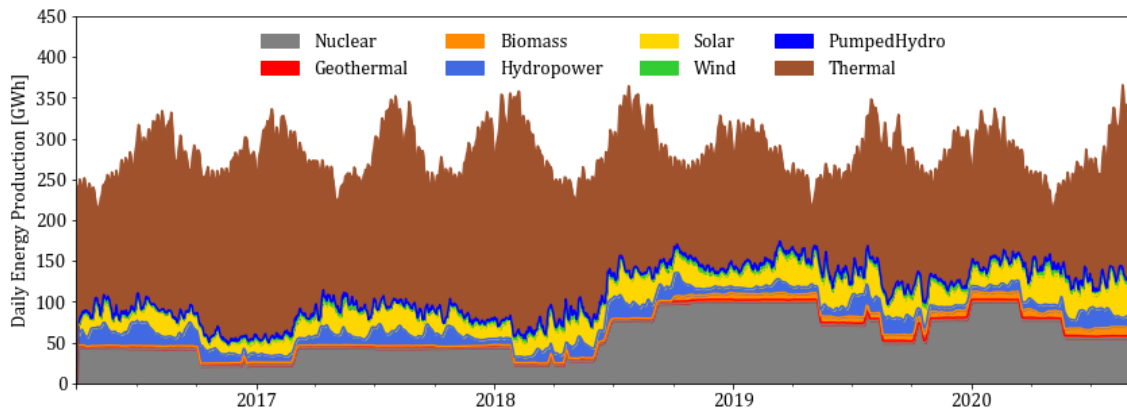


Figure 1. Energy Production of Kyushu Published by Kyushu Electric Power Company.

Figure 2 shows the curtailment profile of Kyushu in March 2019. The area graph shows the total generation of the region from various energy sources. Curtailment is necessary when the overall demand (red line) is below the region’s generation capacity (area graph). The overall demand includes the local Kyushu demand, the transmission, and the charging of the pump hydro. The curtailment’s magnitude (yellow line) already reached 1 GW at peak curtailment during the weekend. Moreover, the figure shows that the pump hydro storage (dark blue) was charged, the transmission (dark green) was increased, and the thermal production (brown) was reduced, but these efforts were insufficient to meet the energy balance. Recent data from October 2019 and March 2020 also show curtailment. Curtailment will eventually increase in frequency and magnitude since the installed solar capacity will continually grow based on the approved solar power plant plans.

Kyushu can generate as much as 20 GW at peak generation; thus, its transmission capabilities to other regions are limited. Kyushu represents island nations with geographically isolated electrical grids like the Philippines, Indonesia, and Hawaii, or technologically isolated grids like South Korea. In these situations, transmission to neighboring countries or grids could not solve the curtailment problem. Storage is the best solution to support the further increase in solar capacity.

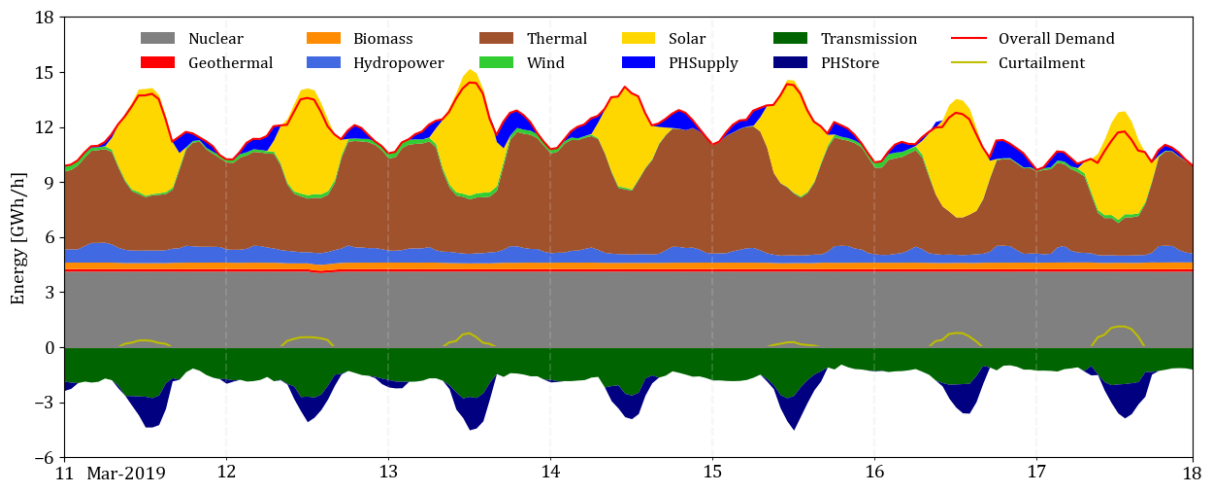


Figure 2. Curtailment Profile in Kyushu in March 2019.

1.3. Electrical Energy Storage

There are several ways to categorize electrical energy storage (EES) such as stored energy type [17], energy conversion interface [18,19], storage mechanism [18,20], and energy storage purpose [21]. Figure 3 categorizes the electrical storage systems based on the conversion interface. Direct electrical storage mainly stores energy via electric fields in capacitors and magnetic fields in inductors without the need for conversion [17,18]. Their use is well-known in electronic circuits, but their capacity to store energy is limited. Electrochemical energy storage utilizes electrochemical reactions to store and produce energy, and the capacity ranges from 100 W to MW [21]. Mechanical energy storage stores energy either through kinetic energy or potential energy [17]. This type of storage produces fewer contaminants throughout its life cycle [20], but its geographical location is its main limitation [21,22].

Chemical energy storage covers technologies where electrical energy produces chemical compounds that could later generate electricity [21]. Electricity can be stored through the production of gas or liquid that could later be used for energy generation or direct utilization [23]. In contrast to the previous three types, the production plant for chemical energy storage is often separate from the generation plant. Thermal energy storage stores energy through temperature change, phase change, or chemical structure change in the material [21]. This kind of energy storage is often used alongside concentrated solar power (CSP) plant for dispatchable generation [24]. Similar to chemical storage, the “charging” and “discharging” interfaces for thermal energy are separate facilities.

Since the theoretical maximum capacity of direct electrical storage is limited, it is infeasible for grid-level storage. The dynamics between the storage and generation of chemical electrical storage may prove to be useful for long-term storage, but since it requires two different facilities, for short-term storage the complexity of the system could hinder its operation; thus, it will not be explored further in this study. Similarly, thermal electrical storage will not be explored further since the current application is limited to CSP. Mechanical and electrochemical electrical storage provides a straightforward conversion between electricity and storage, which is appropriate for diurnal storage. These kinds of storage are essentially built and then cycle through charging and discharging. The capacities of such electrical storage systems are limited mainly by the area and the cost of the installation. The study will mainly focus on these two types of electrical storage.

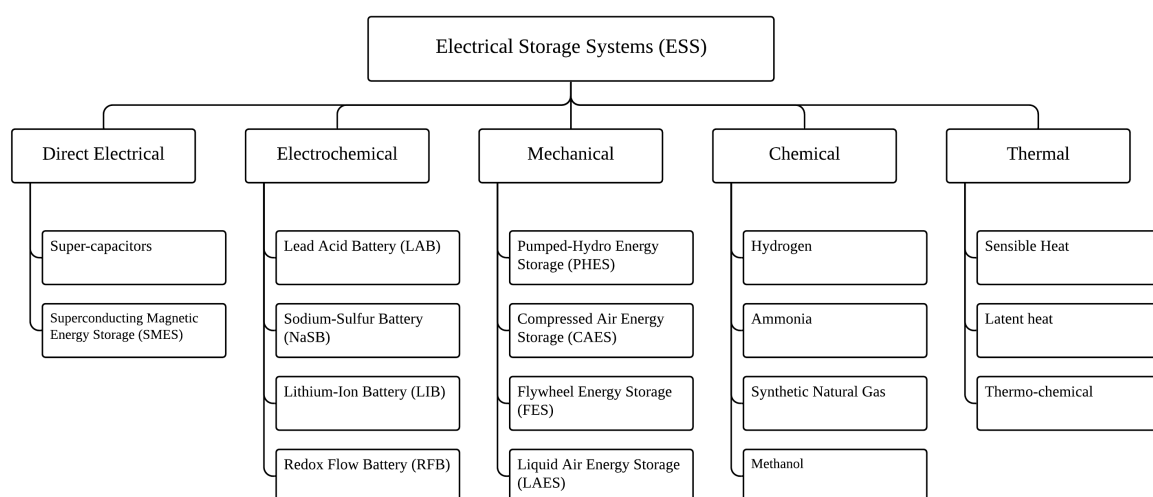


Figure 3. Types of Electrical Storage Systems based on the energy conversion interface. Adapted from [17–21,23].

Pumped hydroelectric energy storage (PHES) requires two reservoirs. It stores energy by pumping water uphill and generates electricity by releasing the water downhill like a typical hydropower plant [21]. It is the most mature and widely used large-scale

energy storage technology, but it is limited by several natural geological features, including adequate elevation and sufficient water supply [21]. Compressed air energy storage (CAES) stores energy by compressing air to high pressures using electrically driven compressors [22]. It generates electricity by allowing the air to expand and mixing the air with fuel in a combustor to drive the turbines [22]. Usually, the compression cycle requires cooling, and the expanding cycle needs preheating [22]. Although it is already considered a developed technology, it suffers the same geographical restrictions of PHES since it requires access to large underground cavities, aquifers, and caverns [22]. Flywheel energy (FES) storage stores electrical energy in the form of rotational energy, but it is designed to deal with short-term voltage disturbance to improve power quality [21]. Liquid air energy storage (LAES) stores energy by storing liquefied cool air in tanks [25]. Electricity is generated by allowing the air to evaporate and drive the turbine [25]. Since it utilizes tanks designed for liquefied air, it does not have geographic restrictions, but its efficiency is low [25].

Lead-acid (PbO_2) battery, although considered to have lower efficiency and energy density, is still used because of its low cost, high reliability and technological maturity [21]. This technology also has a short lifetime at a high depth of discharge, and it requires periodic water maintenance [18]. Sodium sulfur (NaS) battery is one of the batteries used for commercial electrical energy storage in electric utility distribution due to its high energy density, energy efficiency and long cycle capability [21]. However, high capital cost, high operational temperature requirement and high operational hazard limit its application [21]. The increasing number of portable electronic devices has placed a spotlight on Lithium-ion (Li-ion) batteries. Li-ion's high power, energy density, and efficiency make it a potential solution for grid-level storage [19]. However, depending on lithium alone might lead to insufficient supply in the future [26]. Recently, there is an increasing interest in the redox flow battery (RFB) due to its low maintenance cost, overcharging tolerance, and deep charging capability [21], but this technology is still in the development phase [27].

Several studies have summarized the technical and economic properties of existing and potential ESS [18,19,21,28–30]. A recent review by Borri et al. [25] summarizes recent trends in LAES. From these sources, Table 1 summarizes some of the parameters crucial in understanding mechanical and electrochemical storage. Each technology has a different round-trip efficiency, which has an impact on the discharge capacity of the system. To ensure a longer lifetime for some of the batteries (LAB, NaSB, and LIB), they are not completely discharged; thus, only a fraction of their actual capacity is usable. This drawback is not present in mechanical energy storage.

Table 1. Electrical Storage System (ESS) Parameters.

Parameters	Unit	LAB	NaSB	LIB	RFB	PHES	CAES	FES	LAES
Round-trip Efficiency	%	75	80	90	80	75	60	88	50
Discharge Duration		m-h	m-h	m-h	m-h	m-h	m-h	s-m	m-h
Depth of Discharge	%	50	80	80	100	100	100	100	100
Cycle Life	cycle	2000–4500	2500–4500	1500–4500	10,000–13,000	20,000–50,000	>13,000	20,000–100,000	-
Calendary Life	years	5–15	10–15	5–15	5–15	40–60	20–60	15	30–40
Reference		[18,19,28,29]	[18,21,28,29]	[18,21,28,29]	[18,21,28,29]	[18,19,21,28]	[18,19,21,28]	[18,21,28,30]	[25]

The cost of ESS is highly contentious. There are various ways to compute capital expenses and operational expenses. Some authors focus on both the power delivery cost and energy capacity cost [19,21,29,30], while some authors mainly focus on the energy capacity cost and assume a particular duration for the power delivery [31–33]. The former allows more flexibility in the calculations, but the latter simplifies the assumptions in the calculations. Since the focus of this paper is on diurnal storage, the focus will be on the cost of the energy capacity. Schmidt et al. [31] concluded that the capital cost of

ESS systems is on a trajectory towards 340 USD/kWh and 175 USD/kWh for stationary and battery pack storage, respectively, once the total installed capacity reached 1 TWh. They estimated that the storage cost by 2030 would be between 290 USD/kWh to 520 USD/kWh, where PHES and Li-Ion represent the lowest and highest costs, respectively. These conclusions are relatively higher than the projections of Cole and Frazier [32]. After analyzing 25 publications, they concluded that the capital cost of a 4-h battery system would be between 124 USD/kWh and 301 USD/kWh. In Lazard's 2020 Levelized Cost of Storage Analysis [34], they mentioned in their assumption that they used 475 USD/kWh and 102 USD/kWh as their ESS cost for utility-scale PV + storage system. These assumptions are closer to the cost projections of Cole and Frazier for 2020, albeit a pessimistic assumption.

1.4. Economic Assessment

Levelized Cost of Energy (LCOE), calculated by dividing the life cycle cost of the system by its lifetime energy production, is one of the most commonly used economic metrics in comparing energy generators [33]. Early literature stated that it allows the comparison of alternative technologies despite the difference in operational scale, investment, and operating periods [35]. It has become one of the standard economic metrics used in comparing technology, especially in comparing renewable energy with conventional energy (such as coal and Liquefied Natural Gas (LNG)) [36–38]. LCOE is not directly applicable in assessing storage cost since energy storage does not generate its energy. Adapting the basic idea behind LCOE, Jülch et al. [29,39] defined Levelized Cost of Storage (LCOS) as the sum of all the annual expenses (such as operational cost and charging cost) and capital cost divided by the sum of delivered energy over the lifetime of the storage. The approach is relatively similar to LCOE, but instead of generating the energy, LCOS purchases electricity and the delivered energy incorporates the cycle lost (charge and discharge). After examining the LCOS for several ESS technologies, the author highlighted that LCOS is influenced by the design of the storage plant, cost of electricity, and operating hours [29].

Lai and McCulloch [33] focused on a mathematical approach to isolate the LCOS, where storage was seen as separate from the system, and introduced the idea of Levelized Cost of Delivery (LCOD) that provided the relationship between LCOE and LCOS. Schmidt et al. [30] provided a comprehensive analysis of nine storage technologies for several applications and concluded that Li-Ion batteries are the most competitive, and PHES, CEAS, and hydrogen are best for long discharge application.

Storage is starting to be financially viable, and several studies have explored the idea of identifying appropriate storage allocation. Li et al. [40] conducted a technical-economic assessment of large-scale PV integration with PHES in the Kyushu region. PHES was chosen in their study because they evaluated that the topography and geology in the area are favorable to the development of PHES. Their results showed that the additional income from the PV surplus was not enough to cover the additional investment in PHES, but it could offset the initial investment. Anagnostopoulos and Papantonis [41] investigated the performance of pumped storage to support large-scale variable renewable energy in Greece. The authors used the internal rate of return in their economic evaluation and concluded that the project's viability is significantly dependent on the curtailed energy's magnitude and distribution. Liu et al. [42] wrote a review article on energy storage for the electric grid, and in their economic subsection, they mentioned that utility-owned storage provides an excellent opportunity to implement energy arbitrage. Their study highlighted the case of California, but the exact details of the costs and benefits were not disclosed. Nonetheless, the study mentioned that the utility-owned storage systems were making a profit.

1.5. Objective

Most studies consider storage as an additional cost that must be recovered by storing excess solar energy. However, as solar penetration increases further, the cost penalty to solar PV owners due to solar curtailment increases to a point where solar might no longer be economically competitive. At this point, storage is no longer an additional cost but a

necessary infrastructure to maintain solar energy's competitiveness. Consequently, ESS planning should be considered in regions with imminent curtailment issues. There is a need for an optimization approach that provides a target value for the optimal complementary storage capacity in each year, which minimizes the generation cost of renewable energy. This optimization should consider the changes in the cost of ESS and PV and the continuous growth of solar PV. To date, most studies primarily focus on the optimal value for the project and not for the whole system nor for a specific planning horizon. LCOE, LCOS, and LCOD mainly focus on the project's profitability, making it challenging to analyze the impact of additional investments on the existing system. These approaches are well-suited for individual projects but inappropriate for analyzing the whole system, where the capacity of solar and ESS are dynamically changing over several years. Furthermore, these financial assessments are unsuitable for optimization that considers the impacts of early or delayed investments. To the best of the authors' knowledge, an ESS growth trajectory optimization has not previously been explored.

Therefore, this study conducts a techno-economic analysis to present the cost-optimal storage growth trajectory that could support the dynamic integration of solar PV through a particular planning horizon. The optimization aims to balance the cost penalty from curtailment and the additional investment cost of storage. The technical analysis focuses on the energy balance changes due to the increasing solar PV and storage capacity. The economic analysis looks into the changes in the energy generation cost due to solar panel price, storage price, and the utilization rate of the system. A methodology for the cost-optimal assessment is proposed to tackle the time-bound optimization of storage capacity that complements the increasing solar capacity. The proposed approach utilizes a two-step optimization process that performs (a) a technical optimization that maximizes the PV and ESS utilization while ensuring hourly energy balance and (b) an economic optimization that identifies the ESS growth trajectory with the lowest generation cost within the planning horizon. The Kyushu region in Japan was used as a case study since it continuously increases its solar capacity and is at the precipice of high PV curtailment.

The proposed methodology is further discussed in detail in Section 2, including the linear optimization for the hourly energy balance and the Monte Carlo random sampling and financial evaluation for the ESS growth trajectory optimization. The results for the case study are then presented in Section 3, and the implications are discussed in Section 4. Finally, the conclusions are drawn in Section 5.

2. Methodology

Figure 4 shows the overview of the proposed cost-optimal storage capacity assessment, where three process clusters are highlighted. First, the technical optimization focused on maximizing the utilization of the additional ESS from a purely technical perspective. Python for Power System Analysis (PyPSA) Modeling Framework (v0.17.1) [43], which formulates and solves a linear programming problem for optimal power flow, was used to optimize the hourly energy balance. The optimization calculated the energy balance based on various ESS and solar PV capacity scenarios. This calculation was used in the economic optimization, which focused on calculating the optimal growth trajectory. Using the information about the maximum ESS that could support the specified scenarios, the growth trajectory candidates were generated manually and through a Monte Carlo random sampling. The proposed Levelized Cost of Generation (LCOG) was used to provide a financial index for each growth trajectory using financial data about ESS and solar PV and the pre-computed energy balance. The optimal ESS growth trajectory is the trajectory with the least LCOG within the planning horizon. Finally, a sensitivity analysis was conducted to assess the parameters that could affect the trajectory, and an impact analysis was carried out to understand the impact of following the trajectory on the electricity grid.

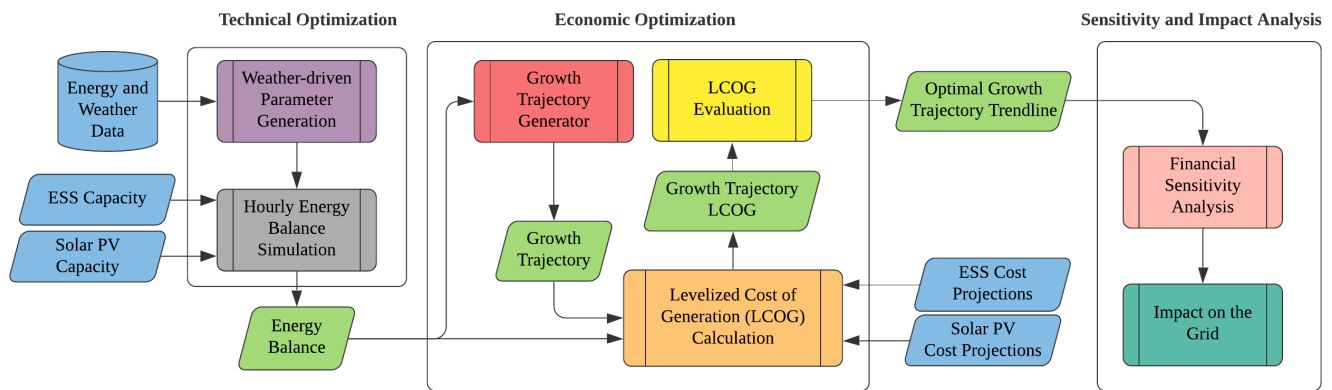


Figure 4. Proposed Cost-Optimal Storage Capacity Assessment using Hourly Simulation, Monte Carlo Sampling, and Levelized Cost of Generation. Blue parallelograms represent the input of the system such as the ESS and PV capacity for the scenarios and the ESS and PV cost projections for the financial calculation. Green parallelograms represent the intermediate output of the processes.

2.1. Technical Optimization

The hourly simulation used Python for the Power System Analysis (PyPSA) Modeling Framework (v0.17.1) [43]. The PyPSA environment provides a framework for the buses, lines, loads, generators, storage, and units, among many other parameters. In this simulation, Kyushu was modeled as a single point, but additional sub-buses were added to monitor the changes in the energy balance due to the additional ESS, as seen in Figure 5. The coal generator was connected directly to the main bus B0 to prevent it from charging the ESS. Since there are still instances when the existing ESS capacity is charged by the other generators, albeit minimal, sub-bus B1 was provisioned to monitor this power flow. B2 was provisioned to monitor the interaction between the PV and ESS. Sub-bus B3 serves as the input for solar and the other generator for the ESS through lines L2 and L3, respectively. Solar has a direct connection to the main bus through line L1, while the delivered energy from ESS goes through L5. For this study, the synthetic load and solar generation profile for the average year (2018) generated in a previous [44] study was used for the optimization. Similarly, the generator parameters seen in Table 2 that were used in that previous study were also used in this study. These generator properties were consolidated based on various sources [45–47]. This study’s solar capacity followed the solar capacity growth in Kyushu from 2012 to 2020, which was detailed in [48]. From the latest published capacity of around 10 GW in 2021 [13], the simulation incremented the PV capacity by 600 MW, 800 MW, and 1 GW per year for the next ten years. The ESS capacity was incremented by 1 GWh from the current 13 GWh capacity until 80 GWh. A preliminary analysis determined 80 GWh as the terminal ESS capacity for the 20 GW solar capacity.

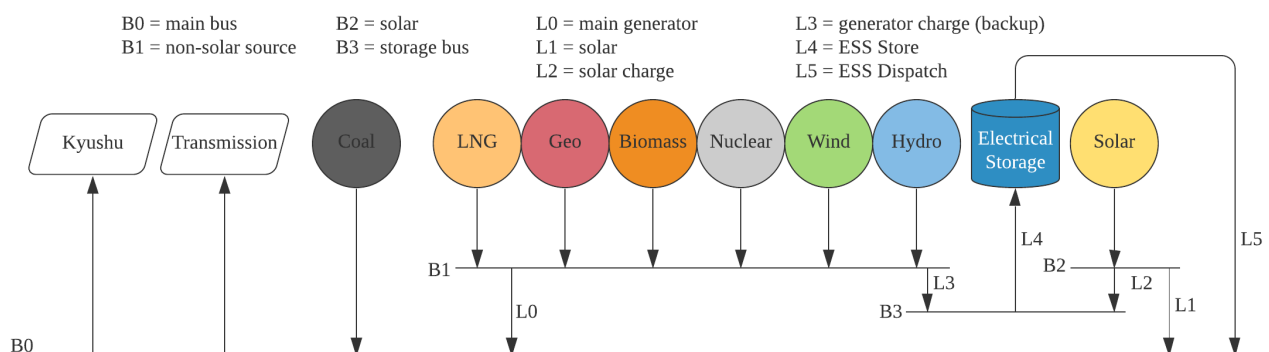


Figure 5. Configuration of the grid used in the optimization.

Table 2. Generators in Kyushu as of FY2019.

Generator	Power [MW]	Carrier	Output _{min} [%]	Ramp Limit [%]
Coal	7037	Coal	30	1
LNG	5250	Gas	15	40
Geothermal	160	Renewable	100	0
Biomass	450	Renewable	100	0
Solar	9000	Renewable	0	100
Nuclear	4140	Non-GHG	100	0
Wind	355	Renewable	15	40
Hydro	4000	Renewable	15	40

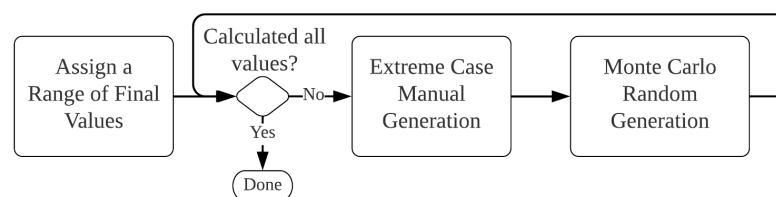
For the optimization, the system prioritizes solar while ensuring energy balance and satisfying the minimum operating output or ramp limit seen in Table 2. Although the nuclear, geothermal and biomass could change within the year, as baseload, it was fixed to its respective maximum capacities to provide consistency throughout the years under simulation. Hydropower generation is based on the daily dispatch capacity calculated using the total daily dispatch in 2019. The simulator allocates the hourly dispatch based on the optimization. However, minimum and maximum dispatch is still considered based on the actual data. The LNG was capped at 10 TWh since this was determined as the current budget in the region in a previous study [44]. Since the analysis focuses on a period of one year, the resulting hourly simulation was consolidated into yearly statistics, which will be used in the economic optimization.

2.2. Economic Optimization

2.2.1. Growth Trajectory Generation

The optimal growth trajectory of ESS is difficult to ascertain due to the enormous amount of potential paths that it could reach. Testing all the paths, even at wide-ranging intervals, seems to be a daunting task. Therefore, this is where Monte Carlo random sampling can be applied. Essentially, this random sampling provides a statistical sample of the available solution space that can identify the optimal solution.

Figure 6 shows the overview of the growth trajectory generation. An initial range of final values was predefined. In this study, the evaluation started from 7 GWh until 67 GWh with intervals of 2 GWh. All these final values go through the manual and random case generation. As outlined in Figure 7, the manual generation, which covers the extreme cases, provides the growth trajectory for single hop, surge, and delay. Single hop focuses on the idea that the planning for the whole duration is conceived at the start, which will dictate the growth trajectory from beginning to end. The surge is similar to the single hop, but the final value is achieved early (e.g., 30 GWh by 2025) and will stay there. On the other hand, the delay scenario will delay the start of the planning (e.g., 0 GWh until 2025) and grow from there. The surge and delay cases were generated from 2021 until 2031 with a 2 year interval. Using these targets, the values in between were interpolated using linear, logarithmic, and exponential growth.

**Figure 6.** Overview of the growth trajectory generation.

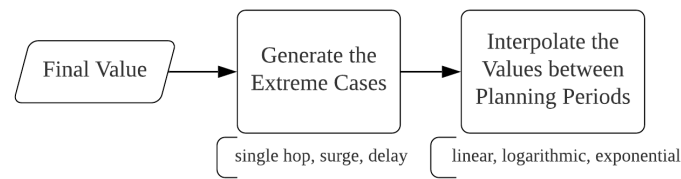


Figure 7. Manual Generation to handle the extreme cases.

Figure 8 outlines the random sampling for the middle cases. The solution space in between the extreme cases is vast, and random sampling reduces the computational requirement of the analysis. However, to ensure that the sampled values represent the whole solution space, it is necessary to approach the sampling methodologically. Similar to the manual generation, the random generation starts with the final value. From this value, planning hops were generated from 2021 until 2031 with a 2 year interval. Table 3 shows the combination of the hops. The sampling rate was identified for each hop length. The number of potential permutations are calculated using the final value and the length of each combination. The growth trajectories were then randomly selected using the target number of samples. Similar to the manual case, the values in between were interpolated using linear, logarithmic and exponential growth. Figure 9 shows a sample growth trajectory using manual generation and random sampling.

Using the specified intervals for the ESS capacity and planning hops, it was determined that there were around five million possible growth trajectories. Following the sampling rate in Table 3, around 430,000 were evaluated. Since there is a possibility of overlap during the generation, the sample size varies depending on the random seed.

Table 3. Planning Hops.

Hops	Number of Hops	Sample [%]
2021, 2023, 2031	3	50
2021, 2025, 2031	3	50
2021, 2027, 2031	3	50
2021, 2029, 2031	3	50
2021, 2023, 2025, 2031	4	10
2021, 2023, 2027, 2031	4	10
2021, 2023, 2029, 2031	4	10
2021, 2025, 2027, 2031	4	10
2021, 2025, 2029, 2031	4	10
2021, 2027, 2029, 2031	4	10
2021, 2023, 2025, 2027, 2031	5	5
2021, 2023, 2025, 2029, 2031	5	5
2021, 2023, 2027, 2029, 2031	5	5
2021, 2025, 2027, 2029, 2031	5	5
2021, 2023, 2025, 2027, 2029, 2031	6	1

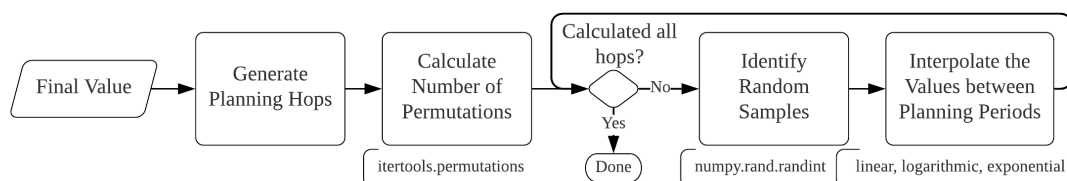


Figure 8. Monte Carlo random sampling for the middle cases.

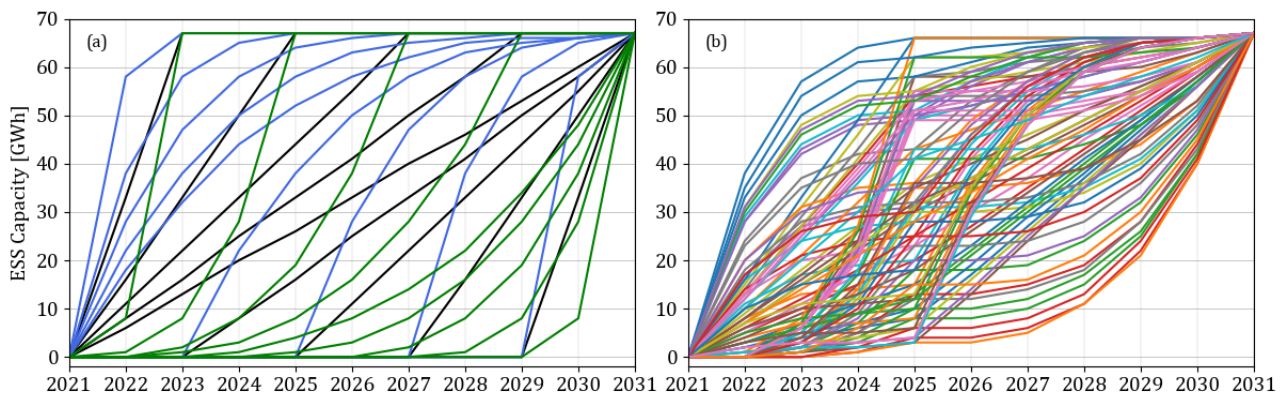


Figure 9. Sample growth trajectory generation using (a) manual generation to handle the extreme cases and (b) Monte Carlo random sampling to provide the random samples in the middle. (a) shows the filling process between planning years, where black, blue, and green represent linear, logarithmic, and exponential growth, respectively. (b) represents one of the planning hops (2021, 2025, 2031) and the filling process as shown in (a).

2.2.2. Financial Evaluation

The proposed Levelized Cost of Generation (LCOG) shown in (1) is used in the financial evaluation of the optimal growth trajectory. The formula is a slight modification of the annuitized Levelized Cost of Energy (LCOE) formula discussed by Lai and McCulloch [33]. Although they did mention that the present value approach is more appropriate in calculating LCOE, to identify the optimal capacity for a particular planning horizon, as is the goal of this work, the annuitizing method is more appropriate since it has to consider additional installation as time progresses. They also emphasized that the variability of solar makes the annuitized formula less appropriate. However, this particular issue is essential in this particular calculation because not only is the energy production variable, with curtailment it is also dependent on the total PV capacity for that particular year. Using LCOE as a foundation, LCOG was formulated by taking into consideration the time component. In contrast to LCOE, which focuses on a unit of energy's production cost for the whole lifetime of the energy generator, the LCOG focuses on a unit of energy's generation cost throughout the planning horizon. This notion facilitates the ability to assess the system as a whole at a certain point in time or a specific period.

$$\text{LCOG}_{y_R}^{\text{PV+ESS}} = \frac{\sum_{y_r=y_{R_0}}^{y_{R_n}} \left(\sum_{y_i=y_0}^{y_n} \left(C_{y_i,y_r}^{\text{PV}} + C_{y_i,y_r}^{\text{ESS}} \right) \right)}{\sum_{y_r=y_{R_0}}^{y_{R_n}} E_{y_r}^{\text{PV+ESS}}} \quad (1)$$

LCOG levelizes the cost of generation within the planning horizon by dividing the total annuitized cost by the total energy generated throughout that period, as seen in the outer summation of the numerator and the denominator. y_R refers to the period under evaluation that begins from y_{R_0} until y_{R_n} . In this study, y_R is 2022–2031, as shown by the bounded box in Figure 10. The inner summation in the numerator represents the cost per year, which is the summation of the annuitized cost of PV and ESS. Since the capital cost changes every year, the annuitized cost will depend on the capacity and annuity in that particular year. The cost is calculated using (2) and (3), where annuity is computed using (4). Japan's interest rate (r) of 3% was used in the calculation. The lifetime of PV and ESS was estimated to be 20 and 15 years, respectively, in this study. Each box in Figure 10 represents an annuity cost either from PV or ESS. The sum of the boxes with the bounding box represents the total cost for the duration of the planning horizon.

$$C_{y_i}^{\text{PV}} = Cap_{y_i}^{\text{PV}} A_{y_i}^{\text{PV}} \quad (2)$$

$$C_{y_i}^{ESS} = Cap_{y_i}^{ESS} A_{y_i}^{ESS} \tag{3}$$

$$A_y = P_y \left[\frac{r(1+r)^n}{(1+r)^n - 1} \right] \text{ (used for both PV and ESS).} \tag{4}$$

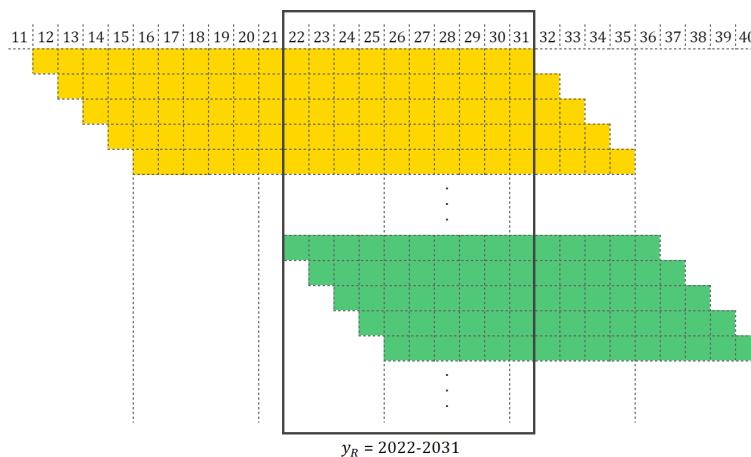


Figure 10. Visualization of the elements of the LCOG. Each box represents an annuity cost either from PV (yellow) or ESS (green). The bounded box represents the planning horizon in this study.

The cost projections for PV and ESS can be seen in Figure 11. The unit cost of solar for each year was used to compute for the annuity ($A_{y_i}^{PV}$) from the principal cost ($P_{y_i}^{PV}$) using (4). In the case of Japan, aside from the panel, there are minimal cost changes; thus, the projection focused on the reduction in PV panel price. A 10% learning curve per year was used since this is the current cost reduction trend. The study assumed that this would continue until 2031. The unit price or principal cost of ESS ($P_{y_i}^{ESS}$) was taken from Cole and Frazier [32], since their projections already considered several publications and they provided the corresponding values for each year while other references only focused on specific years. For the initial calculation, the middle projection for the ESS unit cost (ESS_{mid}) was used. Since the computation used JPY, this was converted from USD to JPY using the current conversion of 1 USD = 110 JPY.

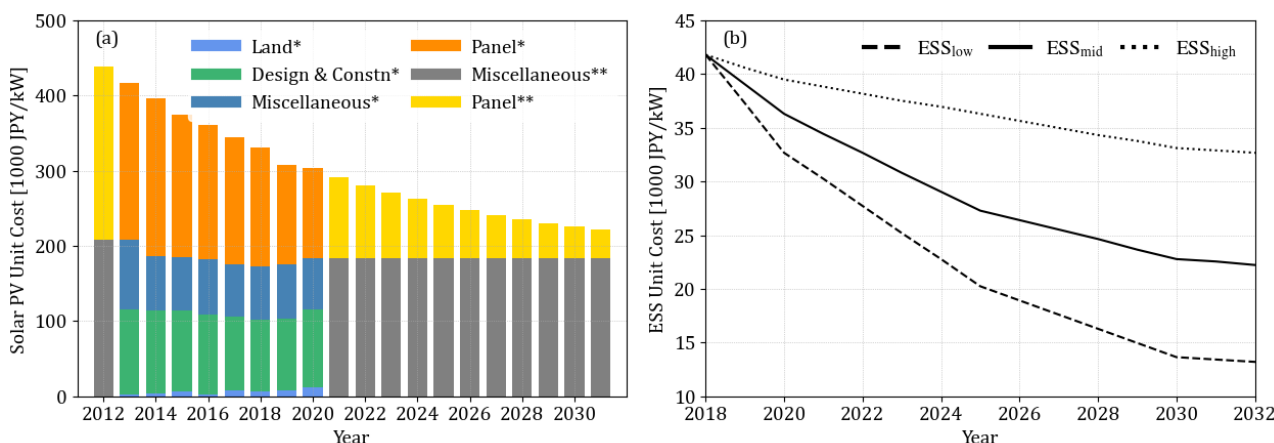


Figure 11. Cost projections for the unit cost of (a) solar PV and (b) ESS. In (a), * is the historical data from Japan’s Ministry of Economy, Trade and Industry [49], where the unit cost is disaggregated into land, design and construction, miscellaneous, and panel price. For the projected values (labeled with **) from 2021 onwards, the land, design and construction, and miscellaneous fees (combined as miscellaneous **) were expected to have minor changes, while the solar panel would continuously decrease by 10% per year. The value for 2012 was also extrapolated since the available historical data started in 2013. (b) shows the cost projections of Cole and Frazier [32] for battery storage with three cost reduction scenarios.

2.2.3. Levelized Cost of Generation (LCOG) Evaluation

At this stage, the LCOG of the candidate growth trajectories were evaluated to extract the optimal growth trajectory. Primarily, the goal was to identify the growth trajectory that yields the minimum LCOG. Secondly, the variations against the other potential solutions were analyzed to assess the impact of not achieving the optimal target. Preliminary analysis showed that several growth trajectories have a relatively similar LCOG compared to the optimal growth trajectory. It was also observed that, for each ESS capacity by 2031 (ESS_{2031}^{cap}), there is a local optimal value. Looking into the 100 samples with the lowest LCOG, it was also observed that the candidates have relatively similar growth trajectories. These trajectories with the lowest LCOG per ESS_{2031}^{cap} were selected as representatives, and a trend line was created using these values. The final goal of the economic optimization is the identification of the trajectory with the minimum LCOG as shown in (5). This goal is achieved at this stage by selecting the candidate trajectory with the lowest LCOG. The ESS capacity trajectory is considered the exogenous variable in this optimization since the model predetermines the other variables.

$$\min \left(LCOG_{yR}^{PV+ESS} (Cap_{y_i, y_r}^{ESS}) \right) \quad (5)$$

2.3. Analysis & Recommendation

2.3.1. Financial Sensitivity Analysis

A sensitivity analysis was conducted to assess the impact of the solar growth rate and ESS unit cost projection on the optimal growth trajectory. For PV, the growth rate was varied under the assumption that larger PV capacity leads to larger curtailment that will require more ESS. In the past three years, PV was increasing by around 1 GW, but it slowed down due to curtailment; thus, 800 MW/year was seen as the realistic case. However, it is ideal to reduce it further to 600 MW/year to slow down the curtailment rate. Consequently, maintaining the 1 GW/year growth is undesirable since it will have the reverse effect. For the ESS unit cost, the projections in Figure 11b were explored to test the robustness of the optimal growth trajectory against the unit cost of storage.

2.3.2. Impact on the Grid

The LCOG for the whole grid includes the other generators. These were treated as dispatchable generations, and the cost was calculated based on the generated amount and the estimated cost as seen in Table 4. It is assumed that there will be minor changes in the price of the other generators in the next decade.

Table 4. Cost of Electricity Generation [Yen/kWh].

Technology	METI 2014	METI 2030	MOFA 2018 *	Applied **
Nuclear	10.1	10.1	-	10.1
Coal	12.3	12.9	6	12.3
LNG	13.7	13.4	10	13.7
Wind	21.9	13.9	10–22 (15)	17.9
Geothermal	19.2	19.2	-	19.2
Hydro	11.0	11.0	-	11
Biomass	12.6	13.3	-	12.6

* Values in parentheses are the average values, ** Used in the calculation.

For the CO₂ emission analysis, the study mainly focuses on the CO₂ emission from fuel consumption, which does not cover the CO₂ emission during the construction, maintenance, and disposal of the system. The calculation assumes that nuclear, geothermal, hydro, solar, and wind does not generate CO₂ and biomass has a net-zero CO₂ emission during electricity generation. According to Japan's Ministry of Environment [50], depending on the technology, coal and LNG has a CO₂ emission of 0.95 kgCO₂/kWh to 0.83 kgCO₂/kWh

and 0.51 kgCO₂/kWh to 0.36 kgCO₂/kWh, respectively. The average emissions for coal (0.89 kgCO₂/kWh) and LNG (0.44 kgCO₂/kWh) were used in the analysis.

To compute the annual generation cost, (1) is slightly modified to incorporate the cost of the other generators. Since the focus is on a particular year, instead of a range (y_R), the focus is on a particular year (y_r). The cost and energy calculations for the combined PV and ESS system are the same, but the calculation now includes the cost and energy from the other technology that contributes to the grid as shown in (6). Since the other technologies are treated as dispatchable energy sources, the cost is computed based on the technology's LCOE and the actual generation that year as shown in (7). The Levelized CO₂ emission was calculated using (8) and the CO₂ emission per technology.

$$\text{LCOE}_{y_r}^{\text{grid}} = \frac{\sum_{y_i=y_0}^{y_n} (C_{y_i,y_r}^{\text{PV}} + C_{y_i,y_r}^{\text{ESS}}) + \sum_{\text{tech}_i=\text{tech}_0}^{\text{tech}_n} C_{y_r}^{\text{tech}_i}}{E_{y_r}^{\text{PV+ESS}} + \sum_{\text{tech}_i=\text{tech}_0}^{\text{tech}_n} E_{y_r}^{\text{tech}_i}} \quad (6)$$

$$C_{y_r}^{\text{tech}_i} = \text{Gen}_{y_r}^{\text{tech}_i} \text{LCOE}^{\text{tech}_i}. \quad (7)$$

$$\text{Levelized CO}_2 \text{ Emissions} = \frac{\sum_{\text{tech}_i=\text{tech}_0}^{\text{tech}_n} (\text{Gen}_{y_r}^{\text{tech}_i}) (\text{Emission}_{y_r}^{\text{tech}_i})}{\sum_{\text{tech}_i=\text{tech}_0}^{\text{tech}_n} \text{Gen}_{y_r}^{\text{tech}_i}}. \quad (8)$$

3. Results

3.1. Energy Change

Figure 12 shows the changes in the solar energy delivered to the grid. It can be seen that, aside from the stored solar, the delivered solar also increased because of the flexibility afforded by the storage. Similar to LNG, it is shown that storage can provide flexibility that could help reduce the ramp rate of the other energy sources. The figure also shows the energy loss due to the charging and discharging cycle (cycle loss), which increases as the amount of ESS capacity increases. The figure also served as a preliminary insight into the maximum ESS capacity for the simulation, since it shows that curtailment will become minimal once 80 GWh was reached.

3.2. Optimal Growth Trajectory

The initial exploration of the sampled growth trajectories showed that the first 100,000 samples have a marginal difference with the minimum LCOG. The calculation showed that, depending on the ESS capacity by 2031 (ESS_{2031}^{cap}), there is a growth trajectory that could yield a relatively similar LCOG, which shows that there is a range of acceptable growth trajectories. Figure 13a shows the 100 trajectories with the lowest LCOG for several ESS_{2031}^{cap} and it can be observed that, for ESS capacities greater than 15 GWh, the LCOG of the trajectories are almost the same. The trajectories with the lowest LCOG for each ESS_{2031}^{cap} are also shown in the figure. Within this trend line, the optimal growth trajectory has the lowest LCOG and is marked as the minima.

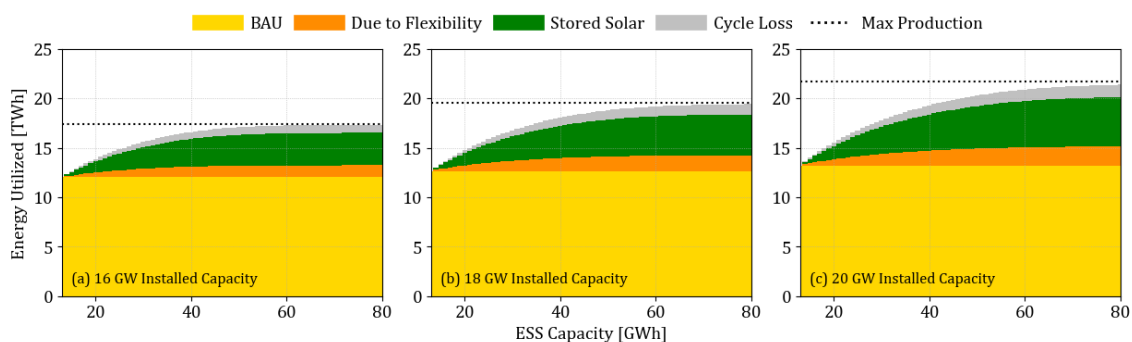


Figure 12. Changes in the total contribution of energy from the combined solar and ESS system.

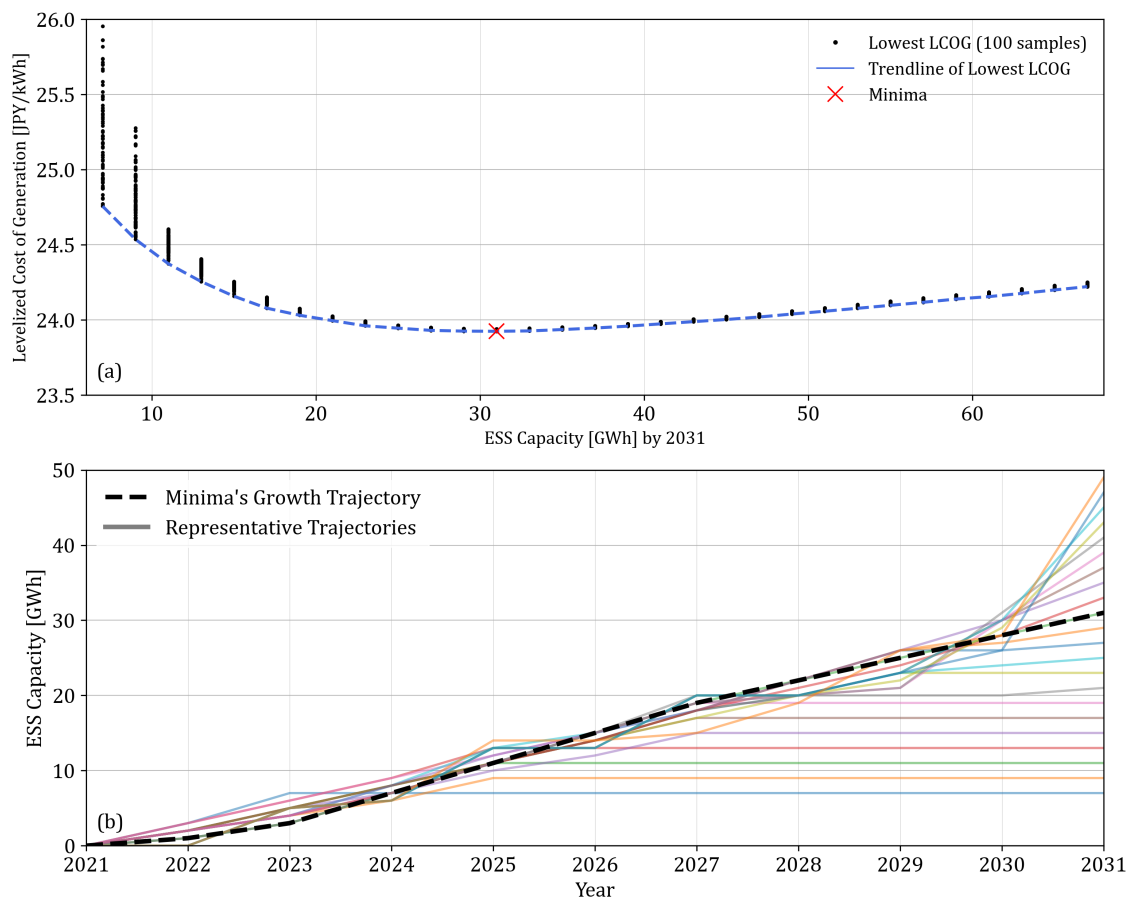


Figure 13. (a) Minimum LCOG per max ESS capacity in 2031. (b) Growth trajectory of the samples with the lowest LCOG sorted according to the ESS capacity by 2031 (ESS_{2031}^{cap}). In (b), the minima's (optimal) trajectory is shown as a dashed line and the representative trajectories are shown as faded solid lines.

Figure 13b shows the representative trajectories and the optimal growth trajectory, where it could be seen that the optimal growth trajectory follows an almost linear trend. The representative trajectories generally follow the optimal trajectory until the maximum ESS capacity for that trajectory is reached. The representative trajectories mainly follow the optimal path until it faces a restriction, which in this case is the maximum assigned capacity for that trajectory. The behavior signifies that the initial goal is to reach the optimal trajectory and retain that capacity until further funding is available. It also shows that investing higher than the optimal trajectory is counter-productive.

3.3. Sensitivity Analysis

The sensitivity of the LCOG and the optimal growth trajectory to the growth rate of solar and changes in ESS unit cost can be seen in Figure 14. As seen in Figure 14a, in all cases, the LCOG gradually decreases but the change for the ESS_{high} is minimal. In contrast, the LCOG for the ESS_{low} drops until it reaches 30 GWh. The minima for lower solar growth rate (e.g., PV_{600}) occurs earlier since there is less curtailment to store. On the other hand, since higher solar growth rates (e.g., PV_{1000}) lead to higher curtailment, the minima are higher since the utilization rate of the ESS remains high, even at these capacity ranges.

Cross-referencing with the corresponding growth trajectory of each minimum shown in Figure 14b, it can be seen that initially, the growth trajectory is the same, but it diverges around 2024. There are points of intersection for the growth rate, but the solar capacity and ESS cost significantly affect the slope of the growth trajectories. Figure 14b also shows that the trend flips around in 2023 and 2024. Initially, the optimal trend for ESS_{high} is higher than the other cases, but its overall slope is less steep. In contrast, the other cases have

lower initial values, but, given their higher slopes, these cases reached higher values by 2031. These trends show that, for instances where the cost reduction is minimal (ESS_{high}), it is best to invest early and immediately reduce the impact of curtailment. However, for instances where cost is seen to drastically reduce in the future (ESS_{low}), it is best to delay. It can also be observed that higher solar capacity growth rates lead to higher required ESS since more curtailment should be recovered. This insight is already intuitive, but it is difficult to assess the capacity and duration of the delay. The optimal growth trajectory presents the capacity to be installed at the minimum to balance the loss and additional investment.

3.4. Impact on the Grid

The analysis of the impact on the grid focused on the average case using the optimal ESS capacity in Figure 14. Since the focus of the optimization is financial, there will still be some curtailment. However, as shown in Figure 15a, the curtailment rate, which is expected to increase continuously, could be kept at around 5–12% through the optimal growth trajectory. It can be observed that the curtailment rate immediately dropped to 12% for ESS_{high} and remained there. In contrast, the curtailment rate gradually reduced to 5% in ESS_{low} and settled there. This observation shows that (a) the lower the cost, the more curtailment can be absorbed and (b) the acceptable curtailment rate will depend on the cost of storage.

Figure 15b shows the annual LCOG using the optimal ESS growth trajectory. It can be seen that the ESS can reduce the curtailment penalty by up to 4–6 JPY/kWh by 2030. The annual LCOG trend follows the trend of the curtailment rate. The LCOG quickly dropped in ESS_{high} and remained relatively high compared to the slower but continuous drop for ESS_{low} .

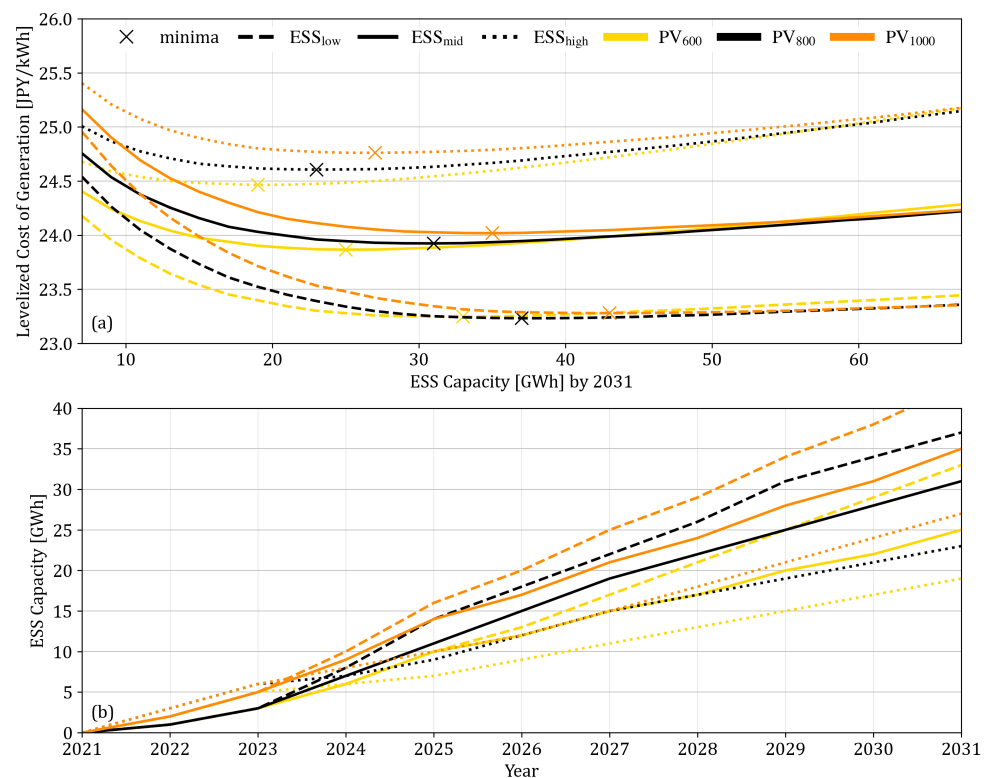


Figure 14. Impact of the solar capacity growth rate and ESS unit cost on (a) LCOG trend line and (b) the cost-optimal growth trajectory. Convention: the color of the line represents the solar capacity growth rate, while the line style represents the project ESS unit cost.

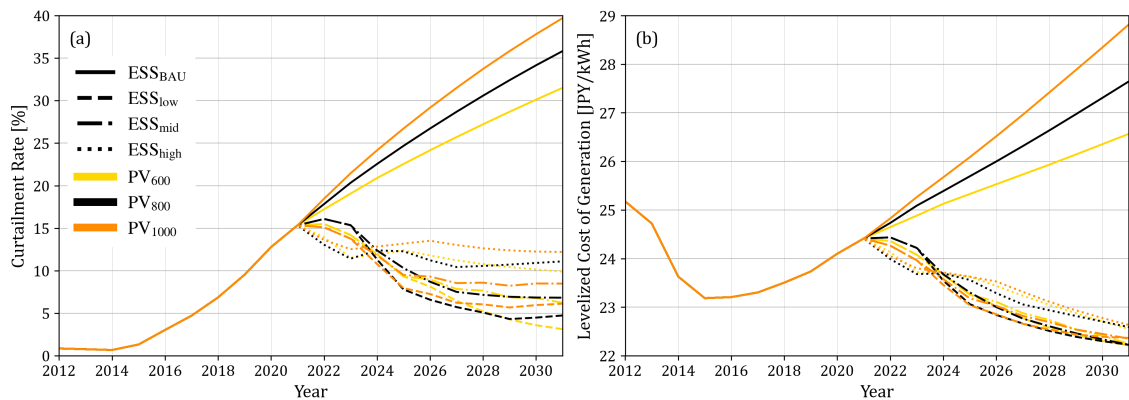


Figure 15. (a) Curtailment rate of solar and (b) Levelized Cost of Generation of the business as usual (BAU; no change in ESS capacity) and the optimal ESS scenario.

The total annual cost of electricity generation for the whole of Kyushu is shown in Figure 16a. Immediately, the impact of additional solar capacity on the annual generation cost is noticeable. It can be observed that, in all cost scenarios, additional storage was able to reduce the annual generation cost. Interestingly, the cost reduction for the three ESS cases is relatively similar. This observation shows that the optimization mainly focuses on the overall impact on the cost reduction. For ESS_{high}, the reduction to a 10% curtailment rate was sufficient to almost match the 5% reduction of ESS_{low}. However, it can be seen that the impact on the CO₂ emissions is more significant, as seen in Figure 16b. Intuitively, higher PV capacity will lead to lower emissions and, since the delivered solar could increase with the aid of ESS, the emissions decrease further. As previously highlighted in Figure 12, aside from the energy delivered through the ESS, the ESS also provides additional flexibility to the grid. These two benefits of ESS reduced the need to generate energy from coal, which leads to a reduction of CO₂ emissions. With the help of ESS, 2–6 million tons of CO₂ could be avoided per year by 2030.

Finally, Figure 17 shows the relationship of the annual LCOG and the levelized CO₂ emissions. As previously highlighted, ESS could slightly reduce the LCOG, but it greatly helps in reducing the CO₂ emissions. By focusing only on solar, the levelized CO₂ emissions could go down to 0.3238–0.3342 kgCO₂/kWh, but with the aid of ESS, this could go down further to 0.2753–0.2825 kgCO₂/kWh. The figure also shows the complementary benefit for PV and ESS in reducing curtailment. A higher solar growth rate and lower ESS unit cost generally lead to lower CO₂ emissions, leading to higher costs. Therefore, a policy decision must be made to balance the power generation's economic and environmental impacts on the island.

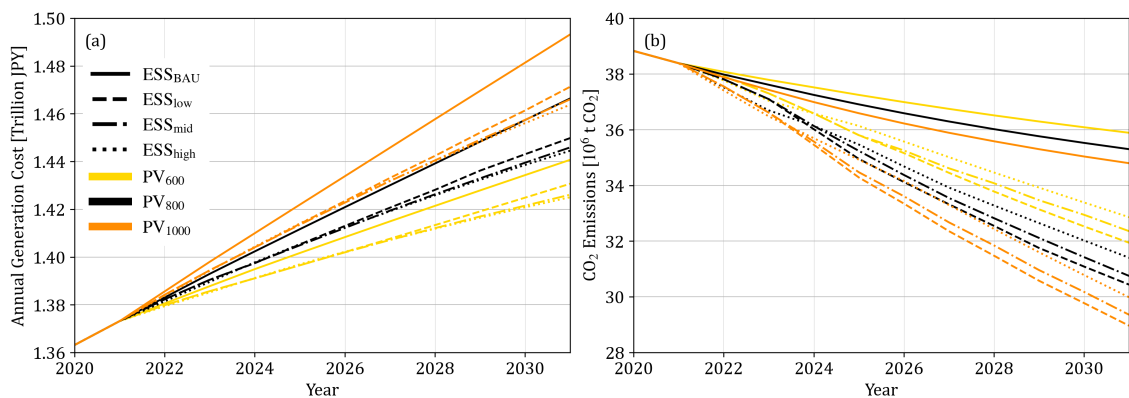


Figure 16. (a) Total annual cost and (b) CO₂ emissions of the electricity generation for the whole Kyushu grid of business as usual (BAU; no change in ESS capacity) and the optimal ESS scenario.

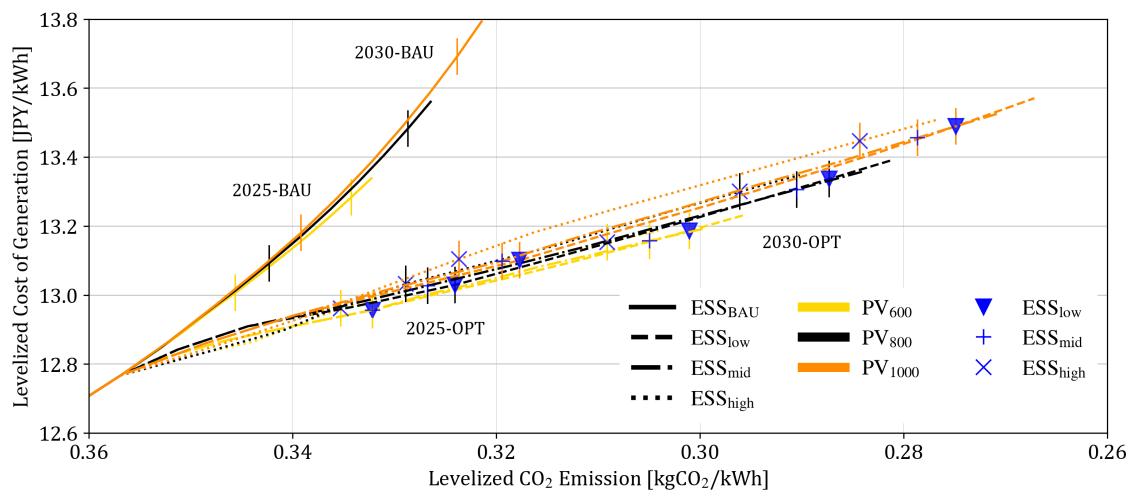


Figure 17. Ratio of the annual Levelized cost of generation and levelized CO₂ emissions for the various scenario. The CO₂ emissions (abscissa) are formatted in decreasing order to emphasize the trend. The additional blue markers show the values for 2025 and 2030 for the different scenarios.

4. Discussion

4.1. Ensuring Continuous Competitiveness of Solar

Curtailment is inevitable under high PV penetration; thus, additional precautions and planning are necessary to minimize its economic impact, which might hinder further deployment of PV. The results show a cost-optimal storage capacity that could reduce the curtailment rate to acceptable levels. Furthermore, results show that there is an optimal growth trajectory for reaching the optimal capacity. By following this growth trajectory, the curtailment rate, which grows larger and larger as the PV penetration rate increases, could be reduced to around 5–10%. Since the optimization focuses on the financial objective, the 5–10% curtailment rate seems acceptable and should be part of the initial cost calculation for new projects. Beyond this curtailment rate, it is financially sound to invest in ESS.

4.2. Solar Energy and Its Impact on CO₂ Emissions

The results also show that, although solar alone can reduce CO₂ emissions, curtailment hinders it from having a more significant impact since the effective delivered energy is reduced. With the aid of ESS, the delivered energy increases and solar could help in reducing CO₂ emissions by displacing coal. The results emphasized that ESS was also able to provide additional flexibility that enabled direct solar utilization. The flexibility of the grid is vital for solar energy since it is a variable source of energy. It is also essential that ESS can provide this since the charging and discharging cycle introduces energy loss, reducing the total delivered solar energy. Furthermore, it is essential to highlight that these additional CO₂ emissions were achieved with a lower annual generation cost.

4.3. Important of Investment's Timing

The results highlighted the importance of investment timing. As solar capacity grows, so does the expected curtailment, and with it, the need for additional ESS capacity. The analysis explored several logarithmic, linear and exponential growth strategies, and the results show that a gradual increase is still the cost-optimal approach rather than a sudden followed by a slow installation (logarithmic) or a slow followed by a sudden installation (exponential). Hypothetically, the logarithmic growth could be beneficial if the grid is severely lacking in ESS capacity. Nonetheless, it should grow until reaching optimal capacity, following the optimal growth trajectory, and continue a linear growth afterwards. On the other hand, exponential growth might be beneficial if a sudden price drop is anticipated in the future. However, as shown in this study, if the curtailment rate is not

yet severe and the price decrease of ESS is gradual per year, then a gradual increase is the financially sound decision.

4.4. Deployment Responsibility

As shown in the optimal growth trajectory, the ESS capacity should be increased by around 30 GWh within the next 10 years to minimize the curtailment cost penalty. This study is limited by the assumption that the whole system will share the benefit of ensuring the competitiveness of solar energy. Further study is necessary to understand the responsibility of the government and existing market players in ensuring the viability of future solar and storage investments. The support given to initial solar investors should also be given to storage investors. The situation of new solar investors should also be considered since they will be more affected by the curtailment because they are entering the market at a point when curtailment is already expected. One potential solution would be to encourage new solar investors to include storage into their system by providing more subsidies or incentives to complementary solar storage plants.

4.5. Implications for Other Isolated Grids

Kyushu's 2 GW transmission line to the rest of Japan is insufficient for solving the curtailment problem in the region. Therefore, Kyushu could represent island nations with isolated electrical grids such as the Philippines, Indonesia, and Hawaii. The results in this study have shown that curtailment will drastically increase the cost of solar once the curtailment rate reaches 10%, and storage should be strongly considered to mitigate its financial impacts. This insight could serve as a precaution for energy planners since ESS represents an additional investment, which could be prevented by limiting the capacity of solar generation. This approach might be counter-intuitive in the effort to green the grid, but it is crucial to prevent wastage of solar energy, as it impacts its profitability.

However, it should be noted that the difference in solar irradiation and demand profiles have a huge impact on the cost of solar generation. For instance, the Philippines and Indonesia have minor variations in temperature, which could result in stable demand. Both countries also have higher solar irradiance that could offset some of the losses. The proposed cost-optimal storage capacity assessment methodology could be adapted for these territories since the storage cost and installed solar capacity are barely affected by changes in territory.

4.6. Importance and Limitation of the Proposed Approach

The proposed cost-optimal storage capacity assessment revealed the ESS growth trajectory that could minimize the cost of electricity generation from the combined PV and ESS system. Since there are a lot of potential growth paths, the computational requirements are enormous. A significant number of samples were used to find the optimal growth trajectory through the Monte Carlo random sampling approach. The proposed formulation for the LCOG was able to calculate the cost of generation as time progresses, as it is geared towards the actual generation per year. In contrast, the standard LCOE mainly focuses on the lifetime of the project. Through the LCOG, the growth trajectory was analyzed to find the set of cost-optimal growth trajectories.

Since the approach optimizes a certain planning horizon, it is only optimal within that period. It does not look further beyond this period. A longer planning horizon could be explored, but this will further increase the computational requirement. One way to handle this is to reduce the yearly intervals and assume minor changes within 2–3 years. By reducing the intervals, the analysis could also be used for 20–30 years. It might not be logical to increase this further since the difference in installed capacity beyond three years could significantly impact the results.

5. Conclusions

The proposed cost-optimal storage capacity assessment was able to identify the complementary ESS growth trajectory that could support rapid PV capacity growth. By separating the optimization process into a two-step process, the first step ensured that the optimization is technically viable, while the second step identified the ESS growth trajectory with the lowest generation cost. Levelized Cost of Generation (LCOG) was introduced as it could provide the ability to tackle the time-bound optimization of the installed storage capacity. The cost-optimal ESS growth trajectory has the lowest LCOG within the planning horizon. The incorporation of the Monte Carlo sampling significantly reduced the computational requirements of the analysis while ensuring the appropriate representation of the growth paths. In addition, the proposed LCOG calculation was able to incorporate the gradual growth of PV capacity and the changes in the cost, which enabled the optimization within the planning horizon. The results showed that there could be several paths to follow in installing ESS, but there is an optimum growth trajectory that could minimize the generation cost. Regardless of the existing storage capacity, the results showed that the complementary capacity should rapidly increase until the optimal growth trajectory and then continuously follow the trajectory. Investing higher capacity reduces the utilization rate of the ESS, which leads to higher LCOG. The approach effectively identified the appropriate amount and timing for the storage capacity, thereby reducing early or delayed investment repercussions. These insights are essential considerations for energy planners and other stakeholders as it provides target values for each year.

As intended, following the optimal growth trajectory resulted in a decrease in curtailment; however, from a financial perspective, eliminating curtailment is infeasible. In Kyushu's case, the results show that the curtailment could be reduced to around 5–12% by following the optimal growth trajectory. The Levelized CO₂ emissions could decrease from 0.3238–0.3342 kgCO₂/kWh with only PV, to 0.2753–0.2825 kgCO₂/kWh with PV and ESS, by 2030. These results show that once curtailment reaches more than 10%, to maximize solar PV's potential in reducing CO₂ emissions, storage must be included in the energy transition plan. The proposed approach can help identify the optimal ESS growth trajectory, which could balance the acceptance of a certain percentage of solar energy wasted as curtailment and investment in ESS to absorb the curtailment.

Since the proposed approach mainly depends on the hourly simulation, it could be replicated in other territories, provided that the hourly data on demand and solar generation are available. Storage will be crucial in ensuring the competitiveness of solar, especially in isolated territories such as the Philippines, Indonesia, and Hawaii. The approach presented in this study could be used to evaluate the growth trajectories for these territories as well.

Author Contributions: Conceptualization, S.M.G.D. and K.N.I.; methodology, S.M.G.D. and K.N.I.; software, S.M.G.D.; validation, S.M.G.D. and K.N.I.; formal analysis, S.M.G.D.; investigation, S.M.G.D.; resources, K.N.I.; data curation, S.M.G.D.; writing—original draft preparation, S.M.G.D.; writing—review and editing, K.N.I.; visualization, S.M.G.D.; supervision, K.N.I. All authors have read and agreed to the published version of the manuscript.

Funding: This research received no external funding.

Acknowledgments: The authors are grateful for the financial support from the Ministry of Education, Culture, Sports, Science, and Technology of Japan for the doctoral studies of Samuel Matthew Dumlaog at Kyoto University. The authors are also grateful to the Ambitious Intelligence Dynamic Acceleration (AIDA) Program of Kyoto University for their financial support.

Conflicts of Interest: The authors declare no conflict of interest.

Abbreviations

The following abbreviations are used in this manuscript:

CAES	Compressed air energy storage
CSP	Concentrated Solar Power
EES	Electrical Storage System
ESS_{2031}^{cap}	ESS capacity in 2031
LCOD	Levelized Cost of Delivery
LCOG	Levelized Cost of Generation
LCOS	Levelized Cost of Storage
LAES	Liquid Air Energy Storage
LNG	Liquefied Natural Gas
Li-ion	Lithium-ion
NaS	Sodium Sulfur
NPP	Nuclear Power Plant
PHES	Pumped Hydroelectric Energy Storage
RFB	Redox Flow Battery

References

- Martinot, E. Grid Integration of Renewable Energy. *Annu. Rev. Environ. Resour.* **2016**, *223*–254. [CrossRef]
- REN21. Renewables 2020 Global Status Report. 2020. Available online: https://www.ren21.net/wp-content/uploads/2019/05/gsr_2020_full_report_en.pdf (accessed on 8 December 2020).
- Denholm, P.; Margolis, R.; Milford, J. Production Cost Modeling for High Levels of Photovoltaics Penetration. In *Renewable Energy Laboratory Technical Report*; 2008. Available online: <https://www.nrel.gov/docs/fy08osti/42305.pdf> (accessed on 8 December 2020).
- California Independent System Operator. *Energy and Environmental Goals Drive Change*; California Independent System Operator; 2016. Available online: https://www.aiso.com/Documents/FlexibleResourcesHelpRenewables_FastFacts.pdf (accessed on 8 December 2020).
- Denholm, P.; Margolis, R.M. Evaluating the limits of solar photovoltaics (PV) in electric power systems utilizing energy storage and other enabling technologies. *Energy Policy* **2007**, *35*, 4424–4433. [CrossRef]
- Hart, E.K.; Stoutenburg, E.D.; Jacobson, M.Z. The Potential of Intermittent Renewables to Meet Electric Power Demand: Current Methods and Emerging Analytical Techniques. *Proc. IEEE* **2012**, *100*, 322–334. [CrossRef]
- Richardson, D.B.; Harvey, L. Strategies for correlating solar PV array production with electricity demand. *Renew. Energy* **2015**, *76*, 432–440. [CrossRef]
- Lund, P.D.; Lindgren, J.; Mikkola, J.; Salpakari, J. Review of energy system flexibility measures to enable high levels of variable renewable electricity. *Renew. Sustain. Energy Rev.* **2015**, *45*, 785–807. [CrossRef]
- Janko, S.A.; Arnold, M.R.; Johnson, N.G. Implications of high-penetration renewables for ratepayers and utilities in the residential solar photovoltaic (PV) market. *Appl. Energy* **2016**, *180*, 37–51. [CrossRef]
- Pfenninger, S.; Hawkes, A.; Keirstead, J. Energy systems modeling for twenty-first century energy challenges. *Renew. Sustain. Energy Rev.* **2014**, *33*, 74–86. [CrossRef]
- Mansouri, N.Y.; Crookes, R.J.; Korakianitis, T. A projection of energy consumption and carbon dioxide emissions in the electricity sector for Saudi Arabia: The case for carbon capture and storage and solar photovoltaics. *Energy Policy* **2013**, *63*, 681–695. [CrossRef]
- Japan Ministry of Economy, Trade, and Industry. Japan's Fifth Strategic Energy Plan (Provisional Translation). 2018. Available online: https://www.enecho.meti.go.jp/en/category/others/basic_plan/5th/pdf/strategic_energy_plan.pdf (accessed on 18 October 2019).
- Kyushu Electric Company. Supply and Demand Information. 2019. Available online: http://www.kyuden.co.jp/wheeling_disclosure.html (accessed on 28 April 2021). (In Japanese)
- Kyushu Electric Company. Kyushu Electric Company Group Annual Report 2018. 2018. Available online: http://www.kyuden.co.jp/var/rev0/0149/3830/c7ujptmy_all.pdf (accessed on 28 April 2021).
- Kyushu Electric Company. Transmission Line Configuration in Kyushu. 2019. Available online: <https://www.kyuden.co.jp/var/rev0/0240/3791/hgajn6ar.pdf> (accessed on 28 April 2021). (In Japanese)
- Federation of Electric Power Companies of Japan. Electricity Review Japan 2019, 2019. Available online: https://www.fepec.or.jp/library/pamphlet/pdf/04_electricity.pdf (accessed on 8 December 2021).
- Díaz-González, F.; Sumper, A.; Gomis-Bellmunt, O.; Villafila-Robles, R. A review of energy storage technologies for wind power applications. *Renew. Sustain. Energy Rev.* **2012**, *16*, 2154–2171. [CrossRef]
- Kousksou, T.; Bruel, P.; Jamil, A.; Rhafiki, T.E.; Zeraoui, Y. Energy storage: Applications and challenges. *Sol. Energy Mater. Sol. Cells* **2014**, *120*, 59–80. [CrossRef]

19. Das, C.K.; Bass, O.; Kothapalli, G.; Mahmoud, T.S.; Habibi, D. Overview of energy storage systems in distribution networks: Placement, sizing, operation, and power quality. *Renew. Sustain. Energy Rev.* **2018**, *91*, 1205–1230. [CrossRef]
20. Mahmoud, M.; Ramadan, M.; Olabi, A.G.; Pullen, K.; Naher, S. A review of mechanical energy storage systems combined with wind and solar applications. *Energy Convers. Manag.* **2020**, *210*, 112670. [CrossRef]
21. Aneke, M.; Wang, M. Energy storage technologies and real life applications—A state of the art review. *Appl. Energy* **2016**, *179*, 350–377. [CrossRef]
22. Gür, T.M. Review of electrical energy storage technologies, materials and systems: Challenges and prospects for large-scale grid storage. *Energy Environ. Sci.* **2018**, *11*, 2696–2767. [CrossRef]
23. Dias, V.; Pochet, M.; Contino, F.; Jeanmart, H. Energy and Economic Costs of Chemical Storage. *Front. Mech. Eng.* **2020**, *6*. [CrossRef]
24. Kuravi, S.; Trahan, J.; Goswami, D.Y.; Rahman, M.M.; Stefanakos, E.K. Thermal energy storage technologies and systems for concentrating solar power plants. *Prog. Energy Combust. Sci.* **2013**, *39*, 285–319. [CrossRef]
25. Borri, E.; Tafone, A.; Romagnoli, A.; Comodi, G. A review on liquid air energy storage: History, state of the art and recent developments. *Renew. Sustain. Energy Rev.* **2021**, *137*, 110572. [CrossRef]
26. Vikström, H.; Davidsson, S.; Höök, M. Lithium availability and future production outlooks. *Appl. Energy* **2013**, *110*, 252–266. [CrossRef]
27. Doetsch, C.; Burfeind, J. Vanadium Redox Flow Batteries. In *Storing Energy*; Elsevier: Oxford, UK, 2016; pp. 227–246. [CrossRef]
28. Zakeri, B.; Syri, S. Electrical energy storage systems: A comparative life cycle cost analysis. *Renew. Sustain. Energy Rev.* **2015**, *42*, 569–596. [CrossRef]
29. Jülch, V. Comparison of electricity storage options using levelized cost of storage (LCOS) method. *Appl. Energy* **2016**, *183*, 1594–1606. [CrossRef]
30. Schmidt, O.; Melchior, S.; Hawkes, A.; Staffell, I. Projecting the Future Levelized Cost of Electricity Storage Technologies. *Joule* **2019**, *3*, 81–100. [CrossRef]
31. Schmidt, O.; Hawkes, A.; Gambhir, A.; Staffell, I. The future cost of electrical energy storage based on experience rates. *Nat. Energy* **2017**, *2*. [CrossRef]
32. Cole, W.J.; Frazier, A. *Cost Projections for Utility-Scale Battery Storage*; Technical Report; US Department of Energy: Washington, DC, USA, 2019. [CrossRef]
33. Lai, C.S.; McCulloch, M.D. Levelized cost of electricity for solar photovoltaic and electrical energy storage. *Appl. Energy* **2017**, *190*, 191–203. [CrossRef]
34. Lazard. Lazard’s Levelized Cost of Storage Analysis—Version 6.0. 2020. Available online: <https://www.lazard.com/perspective/levelized-cost-of-energy-and-levelized-cost-of-storage-2020/> (accessed on 8 May 2021).
35. Short, W.; Packey, D.; Holt, T. *A Manual for the Economic Evaluation of Energy Efficiency and Renewable Energy Technologies*; Technical Report; National Renewable Energy Laboratory: Golden, CO, USA, 1995. [CrossRef]
36. Lai, C.S.; Locatelli, G.; Pimm, A.; Tao, Y.; Li, X.; Lai, L.L. A financial model for lithium-ion storage in a photovoltaic and biogas energy system. *Appl. Energy* **2019**, *251*, 113179. [CrossRef]
37. Das, M.; Singh, M.A.K.; Biswas, A. Techno-economic optimization of an off-grid hybrid renewable energy system using metaheuristic optimization approaches—Case of a radio transmitter station in India. *Energy Convers. Manag.* **2019**, *185*, 339–352. [CrossRef]
38. Gupta, R.; Soini, M.C.; Patel, M.K.; Parra, D. Levelized cost of solar photovoltaics and wind supported by storage technologies to supply firm electricity. *J. Energy Storage* **2020**, *27*, 101027. [CrossRef]
39. Jülch, V.; Telsnig, T.; Schulz, M.; Hartmann, N.; Thomsen, J.; Eltrop, L.; Schlegl, T. A Holistic Comparative Analysis of Different Storage Systems using Levelized Cost of Storage and Life Cycle Indicators. *Energy Procedia* **2015**, *73*, 18–28. [CrossRef]
40. Li, Y.; Gao, W.; Ruan, Y.; Ushifusa, Y. The performance investigation of increasing share of photovoltaic generation in the public grid with pump hydro storage dispatch system, a case study in Japan. *Energy* **2018**, *164*, 811–821. [CrossRef]
41. Anagnostopoulos, J.S.; Papantonis, D.E. Study of pumped storage schemes to support high RES penetration in the electric power system of Greece. *Energy* **2012**, *45*, 416–423. [CrossRef]
42. Liu, J.; Hu, C.; Kimber, A.; Wang, Z. Uses, Cost-Benefit Analysis, and Markets of Energy Storage Systems for Electric Grid Applications. *J. Energy Storage* **2020**, *32*. [CrossRef]
43. Brown, T.; Hörsch, J.; Schlachtberger, D. PyPSA: Python for Power System Analysis. *J. Open Res. Softw.* **2018**, *6*. [CrossRef]
44. Dumlao, S.M.G.; Ishihara, K.N. Weather-Driven Scenario Analysis for Decommissioning Coal Power Plants in High PV Penetration Grids. *Energies* **2021**, *14*, 2389. [CrossRef]
45. Agency for Natural Resources and Energy. Electric Power Survey Statistical Data. Available online: https://www.enecho.meti.go.jp/statistics/electric_power/ep002/results_archive.html (accessed on 8 January 2021).
46. Ministry of Land, Infrastructure, Transport and Tourism. Japan Power Plant GIS Data. 2007. Available online: <https://nlftp.mlit.go.jp/ksj/jpgis/datalist/KsjTmplt-P03.html> (accessed on 8 June 2020).
47. Japan Beyond Coal. Japan Coal Plant Database. 2020. Available online: <https://beyond-coal.jp/map-and-data/> (accessed on 29 September 2020).
48. Knüpfner, K.; Dumlao, S.M.G.; Esteban, M.; Shibayama, T.; Ishihara, K.N. Analysis of PV Subsidy Schemes, Installed Capacity and Their Electricity Generation in Japan. *Energies* **2021**, *14*, 2128. [CrossRef]

-
49. Ministry of Economy, Trade, and Industry (Japan). Solar PV Domestic Trends: Changes in Capital Costs and Their Composition by Year of Installation (Translated; pg 29). 2020. Available online: https://www.meti.go.jp/shingikai/santei/pdf/063_01_00.pdf (accessed on 8 May 2021).
 50. Ministry of Environment of Japan. Evaluation of CO₂ Emissions of Thermal Power Generation. 2016. Available online: <https://www.env.go.jp/council/06earth/y0613-16/ref06-16.pdf> (accessed on 10 March 2020).